SURFACE AND INTERFACE ANALYSIS
Surf. Interface Anal. 2001; **31**: 131–137

SIA

Output characteristics of stacked CMOS-type active pixel sensor for charged particles

Kazuhide Nagashima,[1]* Takuya Kunihiro,[1] Isao Takayanagi,[2] Junichi Nakamura,[2] Koji Kosaka[3] and Hisayoshi Yurimoto[1]

[1] Department of Earth and Planetary Sciences, Tokyo Institute of Technology, 2-12-1 Ookayama, Meguro, Tokyo 152-8551, Japan
[2] Olympus Optical Co., Ltd, 2-3 Kuboyamacho, Hachioji, Tokyo 192-8512, Japan
[3] Tokyo Technology Co., Ltd, 446-8 Katakura, Hachioji, Tokyo 192-0914, Japan

Received 9 June 2000; Revised 2 August 2000; Accepted 12 October 2000

A stacked CMOS-type active pixel sensor (SCAPS) for charged particles has been developed. The SCAPS is an integral-type detector that has several advantages over conventional systems, including two-dimensional detection, wide dynamic range, no insensitive time, direct detection of charged particles and a high degree of robustness. The output characteristics of the SCAPS for incident charged particles has been analysed both theoretically and experimentally. The relationships between the output voltage of the SCAPS and the number of incident charged particles were formulated by including corrections for the non-ideal characteristics of transistors in a pixel. The fluctuation of output characteristics of the SCAPS was evaluated experimentally by irradiation of secondary 4.5 keV Si^+ ions generated by SIMS. The function was used to determine the number of incident ions into each SCAPS pixel within twice the statistical error. The SCAPS is useful as a two-dimensional detector for microanalysis, such as stigmatic SIMS. Copyright © 2001 John Wiley & Sons, Ltd.

KEYWORDS: detector; solid-state image sensor; charged particle; SIMS

INTRODUCTION

An integral-type solid-state image sensor for charged particles, called the stacked active pixel sensor (APS), has been developed for charged particles.[1] The operational principle of APS is based on detecting the change in the potential of a floating photodiode caused by the irradiation of charged particles. As the APS is composed of a rectangular array of 512 × 490 independent microdetectors named pixels, simultaneous two-dimensional detection for charged particles and for soft X-rays can be achieved. The capabilities of the APS have been demonstrated for ions,[1,2] electrons[3,4] and soft X-rays.[5]

The APS has several advantages over conventional systems, including two-dimensional detection, wide dynamic range, no insensitive time, direct detection of charged particles, constant ion sensitivities among nuclides and a high degree of robustness. The characteristics of the APS are utilized in, for example, two-dimensional microanalysis, especially in isotope analysis using stigmatic SIMS. The isotope ratios of some elements range over six orders of magnitude, whereas the relative isotopic variation in nature is less than several per cent. Thus, two-dimensional detection of isotopes over six orders of magnitude under the same conditions is necessary for the determination of isotopic ratios in natural samples. Integral-type detectors are able to store charges suitable for precise, low-intensity measurements for sufficient time integration, thus reducing statistical errors. Because the APS has no insensitive time and is highly robust, it can also measure both the high and low intensity of incident charged particles simultaneously and with the same analytical conditions without mechanical or electronic damage. Normal pulse-count-type detectors have a limitation on beam intensity.

Recently, a CMOS-type APS having a non-destructive readout capability has been developed.[6,7] The use of the non-destructive readout method results in a strong suppression of the level of APS readout noise. In spite of the attractive features of APS, it was found that the degree of non-linearity between incident ions and the APS output is not negligible in cases of high-precision analysis such as isotopic measurements.[8] The aim of this paper is to demonstrate the output characteristics of APS for charged particles and to propose a method for restoration from non-linearity.

PIXEL STRUCTURE AND OPERATIONAL PRINCIPLES OF THE STACKED CMOS ACTIVE PIXEL SENSOR

Figure 1(a) is a schematic cross-sectional view of a pixel of the stacked CMOS APS (SCAPS). Figure 1(b) is a diagram of the circuit configuration. Each pixel unit consists of a pixel capacitor, C_{PIX}, and three transistors (a readout transistor,

*Correspondence to: K. Nagashima, Department of Earth and Planetary Sciences, Tokyo Institute of Technology, 2-12-1 Ookayama, Meguro, Tokyo 152-8551 Japan.
E-mail: kazu@geo.titech.ac.jp

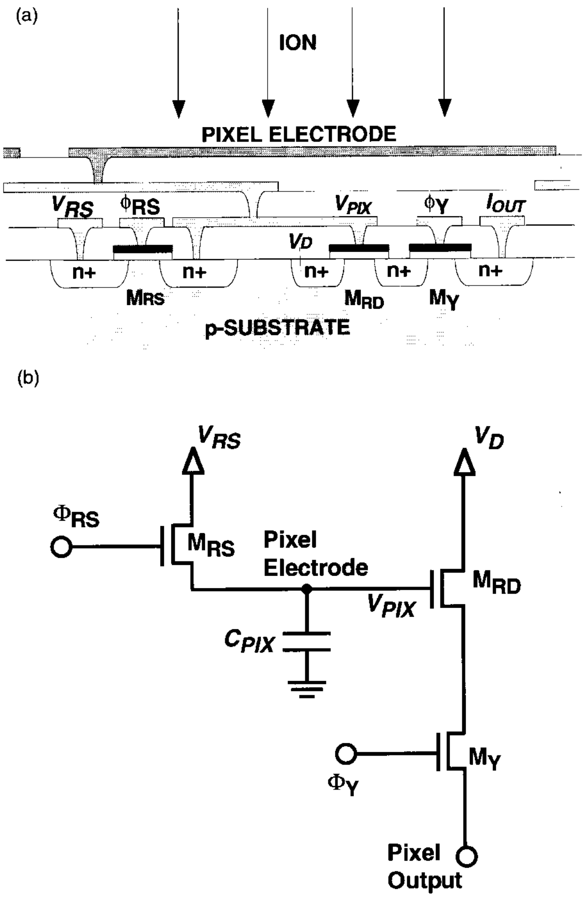

Figure 1. (a) Schematic cross-sectional view of a SCAPS pixel. (b) Circuit configuration of a SCAPS pixel. C_{PIX} = pixel capacitor, V_{PIX} = pixel voltage, V_{RS} = reset voltage, V_D = drain voltage, M_{RD} = readout transistor, M_{RS} = reset transistor, M_Y = column selection switch, Φ_{RS} = reset pulse and Φ_Y = column selection pulse.

M_{RD}, a reset transistor, M_{RS}, and a row selection switch, M_Y). Three metallic layers are stacked on the pixel unit. The top layer, the 'pixel electrode', receives charged particles directly and protects the device underneath. The other two metallic layers are used for electric interconnection and to maintain a flat structure. Because of the separation of the irradiating part and the integrating unit of charged particles, the SCAPS can achieve a high fill factor and detect charged particles regardless of polarity. The SCAPS is designed with pixel dimensions of 14 μm (H) × 14 μm (V) and pixel electrode dimensions of 12 μm (H) × 12 μm (V), thus yielding a fill factor of 73%.

The charged particles irradiated on the pixel electrode release secondary electrons and ions by interacting with the pixel electrode. Some of the incident charged particles are implanted into the pixel electrode. The pixel electrode is thereby electrostatically charged through the interactions. The degree of charging of the pixel electrode is proportional to the number of charged particles. The generated carriers are integrated on the pixel capacitor, C_{PIX}. Accordingly, the SCAPS can store the electrostatic charge until C_{PIX} reaches its maximum capacitance. The basic structure of the SCAPS is principally similar to the stacked amplified MOS intelligent imager (AMI) described by Matsumoto *et al.*[1]

The feature of this pixel structure is that the part detecting the charged particles is separated from the part integrating the carrier. The structure protects the semiconductor part from the high-energy collision of the charged particles and achieves effective carrier transport to the pixel capacitance. Thus, the SCAPS is capable of detection of charged particles in a wide energy range of eV–keV.

The basic operation of the pixel is as follows. After the potential of the pixel electrode, V_{PIX}, is reset to voltage V_{RS} using M_{RS} by a reset pulse, V_{PIX} is changed by the secondary electron emission induced by the charged particle and by the incoming particle itself directly into the pixel electrode. A change of V_{PIX} results in the modulation of the output impedance of M_{RD}. The induced charged particles can be measured by sensing a shift of V_{PIX} from V_{RS}. After the integration period, the signal of the pixel is read through the row selection switch, M_Y. Because the input impedance of the readout transistor, M_{RD}, is very high, the signal charges stored in C_{PIX} are not destroyed and are read multiple times non-destructively until the following reset operation. Signal readouts after the reset operation and without the reset operation are called destructive readout (DRO) and non-destructive readout (NDRO), respectively.[6]

The pixel structures are in a 512 (H) × 490 (V) array. The appearance of the SCAPS device is shown in Fig. 2. The centre area is the imaging area, which measures 7.17 mm (H) × 6.86 mm (V). The pixel array is constructed of a vertical scanner, a horizontal scanner and horizontal selection switches, M_X (Fig. 3). The vertical scanner uses CMOS technology in which NMOS and PMOS devices are combined in a single device.

The CMOS design added two new features to APS. The first additional feature is low power consumption. The average power dissipation is small, of the order of nanowatts. As the number of components per chip increases, power dissipation becomes a major limiting factor in operation. The second additional feature is that the power supply rarely requires close regulation because of the higher permissible voltage.[9,10] Thus, by using CMOS technology, the scanner is capable of operating with an improved level of stable readout.

The vertical scanner has two row buses (row selection and reset). The vertical scanner sends a row selection pulse to a row bus, which connects to M_Y during the horizontal scanning period. When the stored charge of C_{PIX} is reset, the vertical scanner sends a reset pulse to

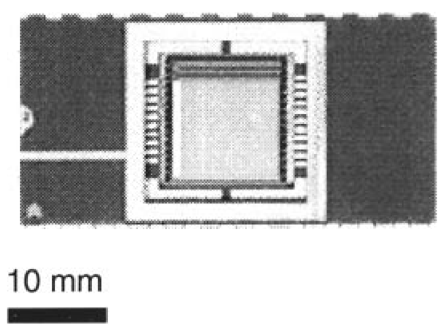

Figure 2. Appearance of SCAPS device.

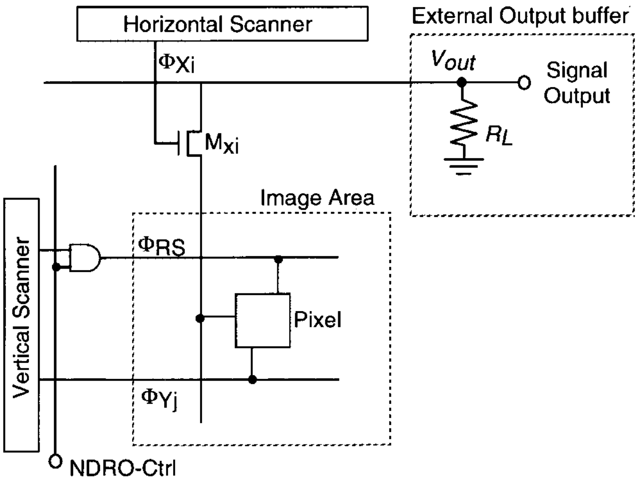

Figure 3. Circuit configuration of SCAPS pixel arrays. M_{Xi} = row selection switch, Φ_{RS} = reset pulse, Φ_{Yj} = column selection pulse, Φ_{Xi} = row selection pulse and R_L = load resistor.

a row bus, which connects to M_{RS}. Switching over from DRO operation to NDRO operation is controlled by an NDRO control signal. Column selection pulses generated by the horizontal scanner are applied to pixels during each horizontal scanning period. Thus, pixels are X-Y addressed and the SCAPS sequentially outputs two-dimensional image information. The signal of the pixel is read as a potential, V_{OUT}, through an off-chip load resistor ($R_L = 20\ k\Omega$), which is located at the end of the horizontal signal line and forms a source follower with the driver transistor, M_{RD}, inside the pixel.

ANALYSIS OF OUTPUT SIGNAL INTENSITY GENERATED BY INCOMING CHARGED PARTICLES

The output voltage, V_{OUT}, relative to the pixel voltage, V_{PIX}, is influenced by the characteristics of the readout transistor, M_{RD}, and a source follower with an off-chip load resistor. In general, the output current, I_{OUT}, of M_{RD} against the pixel voltage, V_{PIX}, is expressed as

$$I_{OUT} = k(V_{PIX} - V_{TH})^2 \tag{1}$$

where k is a coefficient that depends on the pixel size, electron mobility and insulator capacitance per unit size, and V_{TH} is the threshold voltage of M_{RD}.[11] Because I_{OUT} is converted to the output voltage, V_{OUT}, through a source follower with an off-chip load resistor, R_L, in Fig. 3, the relationship between the pixel voltage, V_{PIX}, and the output voltage, V_{OUT}, in an ideal MOS transistor is expressed as

$$V_{PIX} = V_{OUT} + V_{TH} + \sqrt{\frac{V_{OUT}}{kR_L}} \tag{2}$$

which shows that V_{PIX} and V_{OUT} do not have a linear relationship.

To apply the SCAPS to charge particle detection for analysis, it is essential to evaluate the non-linear relationship between the output voltage, V_{OUT}, and incident charged particles, and to establish a method for correcting V_{OUT} to the incident charged particle numbers.

Because the SCAPS is an integral-type detector, the numbers of incident particles, N_i, in a pixel from time t_0 to t_i is expressed as

$$N_i = h(Q_i - Q_0) = h\int_{V_{PIX_0}}^{V_{PIX_i}} C\, dV_{PIX} \tag{3}$$

where h is a transformation coefficient from incident ions to integrated charge in C_{PIX}, and Q and C are the charge and capacitance of C_{PIX}, respectively. Subscripts 0 and i indicate the parameters at t_0 and t_i, respectively. If C can be assumed to be constant, the integrated charges, Q_i, are expressed using Eqn (2)

$$Q_i = C\left(V_{OUT_i} + V_{TH} + \sqrt{\frac{V_{OUT_i}}{kR_L}}\right) \tag{4}$$

Thus, an integrated charge in a pixel capacitor can be calculated from the output voltage, V_{OUT}, using Eqn (4). To cancel the transformation coefficient, h, we introduce a normalized parameter, η, of incident charged particles on a pixel; η_i is defined as

$$\eta_i \equiv \frac{N_i}{N_R} \tag{5}$$

where N_i are the integrated ions from t_0 to t_i and N_R are the integrated ions from t_0 to t_R. Using Eqn (3), η_i is expressed as

$$\eta_i = \frac{Q_i - Q_0}{Q_R - Q_0} \tag{6}$$

where Q_R is the integrated charge at t_R. Because Q_0 and Q_R can be obtained experimentally, they are treated as constants. By substituting Eqn (4) into Eqn (6), η_i is expressed by V_{OUT_i} as

$$\eta_i = \frac{1}{Q_R - Q_0}\left[C\left(V_{OUT_i} + V_{TH} + \sqrt{\frac{V_{OUT_i}}{kR_L}}\right) - Q_0\right] \tag{7}$$

As shown in Fig. 4(a), Eqn (7) basically represents the relationship between η_i and V_{OUT_i}, which was determined experimentally. The methods used for the experimental determination are described later. The errors between the calculated and measured η values are within 10%. The origin of error is due to non-ideal characteristics of the source follower and changes in the capacitance of a pixel caused by variation in the integrated charge.[8] By correcting for the non-ideal characteristics, the formula of Eqn (7) can be modified as

$$\eta_i = a_1 V_{OUT_i} + a_2 + (a_3 V_{OUT_i} + a_4)^{a_5} \tag{8}$$

where a_i are the fitting parameters. From Eqns (5) and (8), the number of integrated ions from t_0 to t_i is expressed as

$$N_i = N_R \eta_i = N_R\left[a_1 V_{OUT_i} + a_2 + (a_3 V_{OUT_i} + a_4)^{a_5}\right] \tag{9}$$

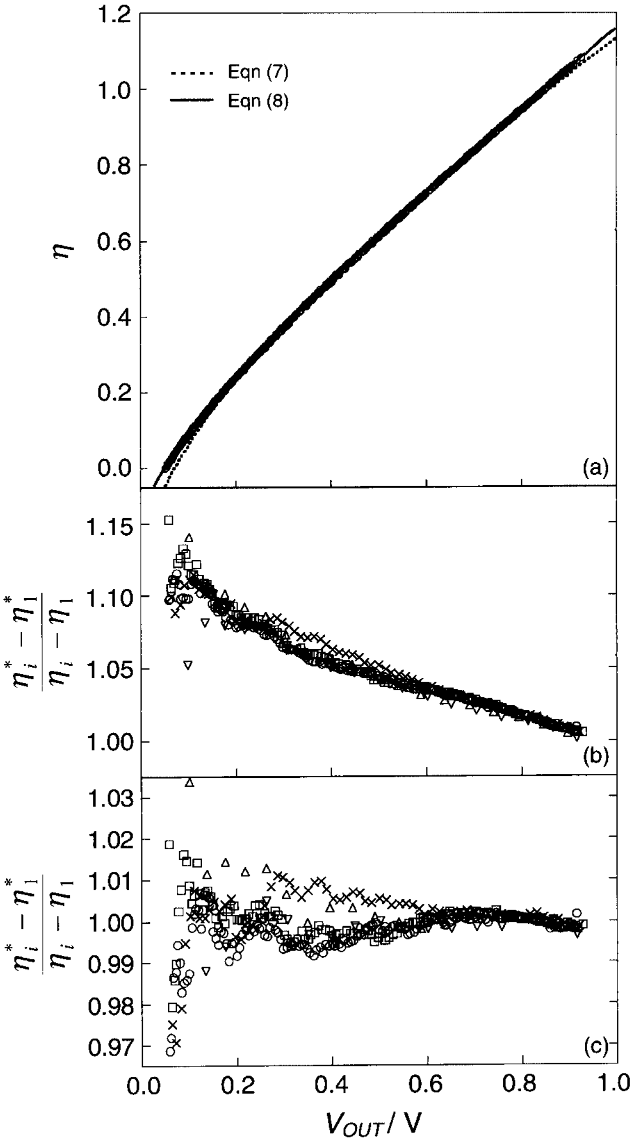

Figure 4. (a) Relationship between output voltage, V_{OUT}, and normalized accumulated ion number, η, of a pixel, Si^+ ions were irradiated onto the SCAPS and η is determined by FC2 monitoring. The regression curves are derived by Eqns (7) and (8). (b) Fitting error of Eqn (7). (c) Fitting error of Eqn (8). (○, □) 200 cps per pixel; (×) 60 cps per pixel; (△, ▽) 30 cps per pixel.

EXPERIMENTAL

Determination of number of incident ions

The output characteristics of SCAPS for charged particles were evaluated by ion irradiation. A schematic configuration of the ion irradiation system and the SCAPS operating system is shown in Fig. 5. Si^+ ions accelerated at 4.5 keV were used as the irradiated charged particles onto the SCAPS. The Si^+ ion beam was generated by a Cameca IMS-3f SIMS instrument. The SCAPS device was placed in an ultrahigh vacuum of <0.5 μPa. Secondary Si^+ ions were generated from a silicon wafer bombarded by 12.5 keV $^{16}O^-$ primary ions. To obtain a homogeneous distribution of the secondary ion emission, primary $^{16}O^-$ ions were rastered over an area of 250 μm × 250 μm, and the secondary Si^+ ions generated in the 60 μm diameter central area were projected directly

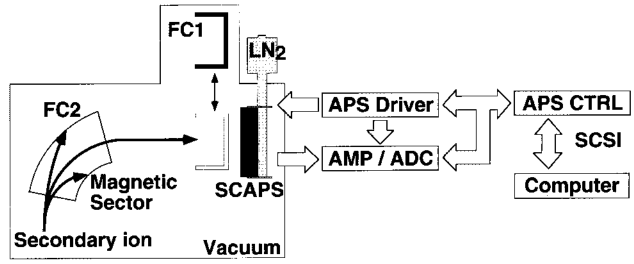

Figure 5. Block diagram of ion irradiation system equipped with SCAPS operating system: LN_2, liquid nitrogen dewar; APS Driver, pulse generator, AMP/ADC, amplifier and analogue–digital converter; APS CTRL, process controller for APS driver and AMP/ADC. Faraday cup, FC1, detects secondary ions passing through a magnetic sector by insertion in front of the SCAPS. The flight tube in the magnetic sector works as Faraday cup, FC2, which detects the total number of secondary ions except for ions passing through the magnetic sector.

onto the SCAPS imaging area using stigmatic ion optics. The projected area covered ~40% of the central field of the SCAPS imaging area, which corresponds to $\sim 10^5$ pixels. The count rate of total secondary ions projected onto the imaging area was measured by insertion of a Faraday cup, FC1, in the IMS-3f instrument. The rate of incoming ions per pixel was calculated by dividing the FC1 intensity counts by 10^5. The calculated rate per pixel includes errors of ion beam fluctuation between the measurement times of the SCAPS and of the Faraday cup as well as statistical errors of the incoming ions themselves.

During the experiments, the fluctuations of secondary ion intensities are often larger than the statistical errors of the ion intensities. The fluctuation of the secondary ion intensity is a serious problem because it adversely affects the precise determination of the integrated ions onto the SCAPS. To determine the count of integrated ions onto the SCAPS, we monitored the secondary ions that were trapped by a flight tube in the magnetic sector of the IMS-3f by a Keithley 6514 electrometer, as shown in Fig. 5. The flight tube, FC2, works as a Faraday cup because its length is long enough to trap charged particles. Therefore, except for the ions passing through the flight tube, the total number of secondary ions can be measured as current. Because the ion species irradiated onto the SCAPS or FC1 are different from the species trapped by FC2, the degree of correlation between the simultaneous measurements by FC1 and FC2 should be evaluated experimentally.

Operation of SCAPS

After ion irradiation, the ion signals from SCAPS were read at a 20 kHz scanning rate per pixel by adding driving pulses to the SCAPS from the APS driver (Fig. 5). The storage time of the ion signals can be selected from 20 s upwards. The signals read from each pixel were amplified and then converted to a digital signal by a 16-bit A/D converter for final processing in a personal computer. To reduce environmental noise, the communications between the SCAPS and the operation electronics were differential signals connected by shielded twisted-pair cables through an ultrahigh vacuum electrical feed-through.

To reduce thermal noise in each pixel during ion irradiation and during the time waiting for the readout, the device was cooled by liquid nitrogen. The SCAPS temperature was held constant at ∼77 K during operation. When the reset transistor, M_{RS}, is used to reset a pixel, a random noise, called the reset noise, is generated. The reset noise of the SCAPS at 77 K is estimated to be ∼25 e^-.[7] To suppress the reset noise, the following NDRO sequence (Fig. 6) was applied:

(1) for imager reset, each pixel is reset by a DRO operation.
(2) For offset frame read, the reset signals of each pixel are read by an NDRO operation. A fixed pattern of noise among the pixels caused by variations of the threshold level of readout transistor, M_{RD}, and by the reset noise are included in the signal.
(3) Charged particles are irradiated on the SCAPS.
(4) For signal frame read, ion-integrated signals are repeatedly read by an NDRO operation during ion irradiation. Subtracting the output of the offset read from the output of the signal read extracts only the accumulated components of irradiated ions on each pixel.

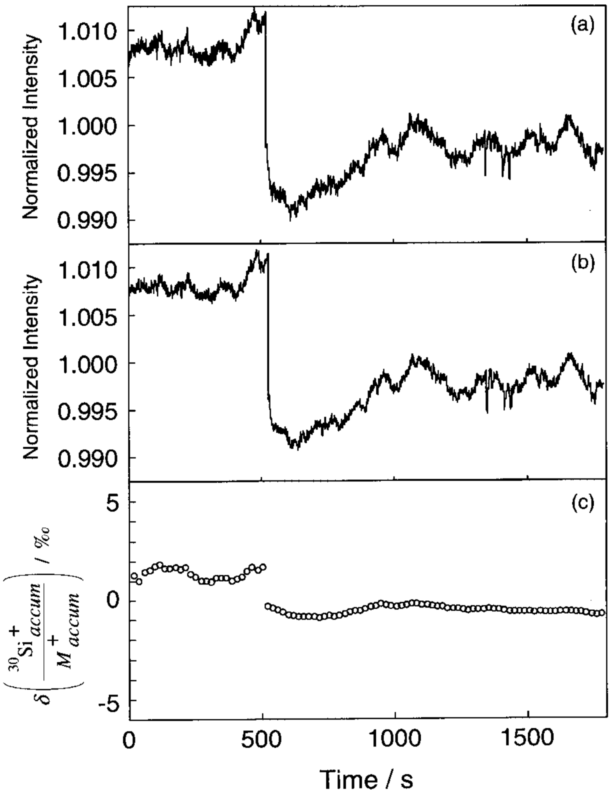

Figure 7. Variation of ion intensities by (a) FC1 monitoring and (b) FC2 monitoring. Ion intensities are normalized by the average intensities. (c) Correlation of accumulated ion intensities between FC1 and FC2 monitoring.

RESULTS AND DISCUSSION

Correlation between incident ion intensity onto the SCAPS and total secondary ion intensity

Typical relationships between simultaneous measurements of ion intensities by FC1 and FC2 are shown in Figs 7(a) and 7(b). The FC1 monitored the $^{30}Si^+$ ion and FC2 monitored other secondary ions. The ion intensities for each Faraday cup are normalized by the average currents through the run. The average currents for FC1 and FC2 are 5.0×10^{-13} and 2.0×10^{-11} A, respectively. The variations of intensities for FC1 are correlated to those for FC2 for >1800 s. Figure 7(c) shows the relative differences of the accumulated ions between the measurements. The relative differences of accumulated ions between the currents for $^{30}Si^+$ by FC1 and for other ions, M^+, by FC2 are expressed as

$$\delta\left(\frac{^{30}\mathrm{Si}^+{}_{\mathrm{accum}}}{\mathrm{M}^+{}_{\mathrm{accum}}}\right) \equiv \left(\frac{\int_0^j {}^{30}\mathrm{Si}^+\,\mathrm{d}t \Big/ \int_0^{1800} {}^{30}\mathrm{Si}^+\,\mathrm{d}t}{\int_0^j \mathrm{M}^+\,\mathrm{d}t \Big/ \int_0^{1800} \mathrm{M}^+\,\mathrm{d}t} - 1\right) \times 1000 \tag{10}$$

where j is an integer from zero to 1800 s. Each point in Fig. 7(c) was calculated from the data shown in Figs 7(a) and 7(b) and plotted every 20 s. The δ values do not increase with time and the overall error for 1800 s is within ±0.15%, including an abrupt intensity shift at ∼500 s. Accordingly, the fluctuation of incident secondary ions irradiated onto the SCAPS can be monitored by FC2 monitoring, i.e. η calculated by FC2 monitoring was within an error of 0.3%.

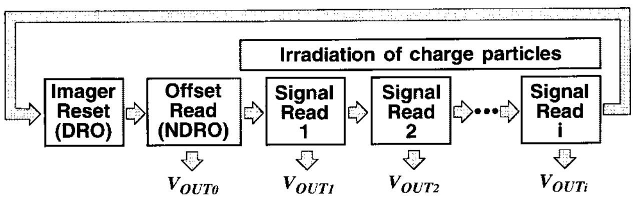

Figure 6. Sequence of signal readout: DRO = destructive readout; NDRO = non-destructive readout.

Evaluation of output characteristics of the SCAPS pixel

The typical relationship between V_{OUT} and η, which was determined by FC2 monitoring, is plotted in Fig. 4(a). The normalization number, N_R, for η was given at $V_{OUT} = 0.85$ V. Therefore, the N_R values among the pixels are different because h in Eqn (3) and the characteristics of the readout transistor, M_{RD}, are slightly different among the pixels. The average N_R among the pixels in this study corresponds to 72 000 ions; the variation of N_R among the pixels is 1.1% (1σ). This means that the variation of ion sensitivity among the pixels is ∼1%.

Five NDRO readout sets of a pixel with different Si^+ currents on the SCAPS are plotted in Fig. 4(a). The average counts of Si^+ in the five sets were 2×10^7 (two runs), 6×10^6 (one run) and 3×10^6 (two runs) counts per second (cps), which corresponds to the average Si^+ intensities in each pixel of 200, 60 and 30 cps, respectively.

All data was plotted along a simple curve. Regression curves for the five sets, η^*, were calculated using Eqns (7) and (8) and are shown in Fig. 4(a). Both curves show good agreement with the output characteristics of SCAPS. To evaluate the fitting error quantitatively, the ratios of η^*

calculated from Eqn (7) or Eqn (8) to observed η are plotted in Figs 4(b) and 4(c). The large errors below $V_{OUT} = 0.1$ V are due to statistical errors of the incident ions. The ratios between η and η^* from Eqn (7) decrease systematically over 10%, depending on V_{OUT}. The systematic changes were analysed as a non-linear response of the SCAPS.[8] The ratios between η and η^* from Eqn (8) are constant for $V_{OUT} = 0$–1 V to within 1%. Thus, Eqn (8) corrects the non-ideal output characteristics of the SCAPS within a 1% error for each pixel.

The parameter range of Eqn (8) for 11×11 pixels in the centre area of the Si irradiation field is shown in Table 1. Although parameter a_5 in Eqn (8) is ideally 0.5, the calculated value of a_5 is 0.22 ± 0.13. This shift is due to the non-ideal characteristics of a source follower and the changing capacitance, depending on the integrated charges in a pixel. The variation of a_5 shows how the degree of non-ideal characteristics changes among pixels. Other parameters for the 121 pixels also varied from pixel to pixel, depending on the non-ideality of the pixel output.

Equation (8) for each pixel determined by the five data sets was applied to another set. The average Si^+ count of the experimental set was 6×10^6 cps, corresponding to the average Si^+ intensity for each pixel of 60 cps. To analyse the cause of the discrepancies between η^* determined by V_{OUT} and η determined by FC2 monitoring of Eqn (8) among the 121 pixels, we introduce $\delta\eta$ as follows

$$\delta\eta_i = \left(\frac{\eta_i^* - \eta_1^*}{\langle \eta_i - \eta_1 \rangle} - 1 \right) \times 1000 \qquad (11)$$

where $\langle \eta_i - \eta_1 \rangle$ is the average of $(\eta_i - \eta_1)$ among the 121 pixels. Each plot of $\delta\eta_i$ in Fig. 8 is the average value among the 121 pixels of SCAPS; the error bar shows the standard deviation among the 121 pixels. The horizontal axis of Fig. 8 corresponds to the accumulated ions from zero to 72 000 because the average N_R is 72 000. The average value of $\delta\eta$ is constant within $\pm 0.5\%$ over the entire range of $\langle \eta_i - \eta_1 \rangle$. The curves in Fig. 8 indicate the theoretical errors of the accumulated ions for a pixel estimated from the counting statistics. The observed standard deviations are nearly equivalent to the statistical errors, but are systematically larger. The components of the standard deviations larger than the statistical errors are considered to be statistical fluctuations of emissions of secondary electrons on the pixel electrodes among the pixels, and the variation of ion sensitivities among the pixels. Although spatial heterogeneity of irradiated ions on the SCAPS is also a possible candidate for an error component, heterogeneity is not likely because the 121 pixels correspond to the centre of the ion-irradiated field and the area is small (140 μm × 140 μm) when compared with the size of the total irradiated field of the homogeneously adjusted beam (4400 μm × 4400 μm).

Table 1. Parameters obtained by a regression curve in Eqn (8)

Parameter	Value ($\pm 1\sigma$)
a_1 (V^{-1})	0.94 ± 0.055
a_2	-0.50 ± 0.22
a_3 (V^{-1})	0.37 ± 0.49
a_4	0.0057 ± 0.0091
a_5	0.22 ± 0.13

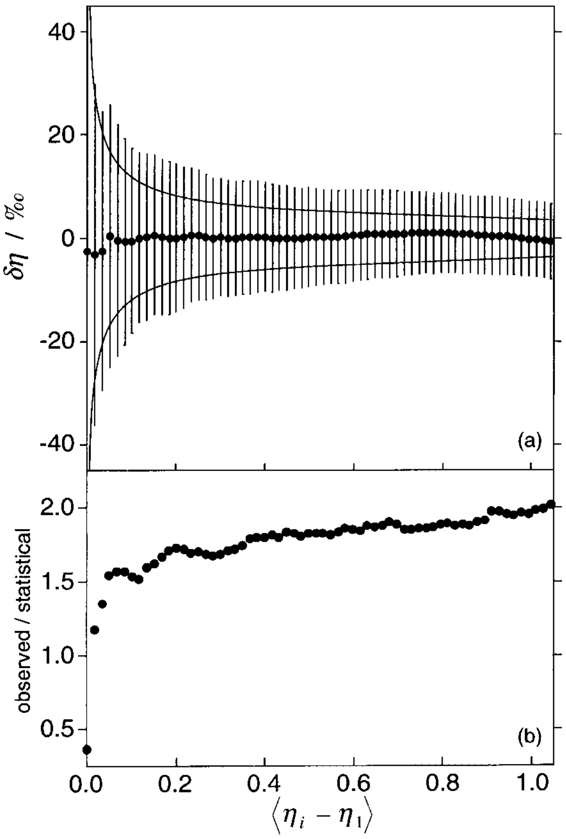

Figure 8. (a) Relationship between $\delta\eta$ and $\langle \eta_i - \eta_1 \rangle$. The plots of $\delta\eta$ are for an average of 121 pixels. The errors are the standard deviations among the 121 pixels. The curves are the statistical errors (1σ) of incoming ions per pixel. (b) Ratios between observed and statistical errors among that pixels against $\langle \eta_i - \eta_1 \rangle$. The observed errors are the standard deviations among the 121 pixels. The statistical errors are estimated from the count statistics.

The ratios between the observed and statistical errors among the pixels are shown in Fig. 8(b). The ratios increase with $\langle \eta_i - \eta_1 \rangle$. This increase is primarily caused by the variation of ion sensitivities among the pixels because the relative variation of sensitivity is constant to $\langle \eta_i - \eta_1 \rangle$ and the other relative errors described above decrease with $\langle \eta_i - \eta_1 \rangle$. Instead of the raw signals, if the signal ratios of each pixel are useful, the differences of ion sensitivities among the pixels can be cancelled. Therefore, the performance-corrected output characteristics are suitable for producing a two-dimensional distribution map of isotope ratios using stigmatic ion optics.

CONCLUSIONS

(1) The variation of accumulated ions on SCAPS was monitored within a 0.3% error range by the measurement of ions trapped in a flight tube in the magnetic sector.

(2) The output signal of a pixel for the SCAPS was corrected to accumulated ion numbers within a 1% degree of uncertainty using the output characteristics

$$\eta = a_1 V_{\mathrm{OUT}} + a_2 + (a_3 V_{\mathrm{OUT}} + a_4)^{a_5}$$

(3) Application of the correction method from output signal to ion numbers is suitable for ion accumulation at least up to 10^5 per pixel. Therefore, the SCAPS is applicable for detectors of two-dimensional quantitative analysis using charged particles.

REFERENCES

1. Matsumoto K, Yurimoto H, Kosaka K, Miyata K, Nakamura T, Sueno S. *IEEE Trans. Electron Devices* 1993; **40**: 82.
2. Yurimoto H, Kosaka K, Matsumoto K, Nakamura T. In *Secondary Ion Mass Spectrometry SIMS IX*, Benninghoven A, Nihei Y, Shimizu R, Werner HW (eds). John Wiley: Chichester, 1994; 258–261.
3. Yurimoto H, Matsumoto K. *Bunseki Kagaku* 1996; **45**: 493.
4. Yurimoto H, Matsumoto K, Kim K, Kitajima H, Kosaka K, Hirata T. In *Secondary Ion Mass Spectrometry SIMS X*, Benninghoven A, Hagenhoff B, Werner HW (eds). John Wiley: Chichester, 1997; 987–990.
5. Takayanagi I, Nagai K, Tetsuka H, Inoue Y, Araki S, Mochimaru S, Iketaki Y, Horikawa Y, Matsumoto K. *IEEE Trans. Electron Devices* 1995; **42**: 1425.
6. Takayanagi I, Nakamura J, Yurimoto H, Kunihiro T, Nagashima K, Kosaka K. *Proc. 1999 IEEE Workshop on Charge-Coupled Devices and Advanced Image Sensors*. 1999; 159.
7. Takayanagi I, Nakamura J, Yurimoto H, Kunihiro T, Nagashima K, Kosaka K. *Tech. Rep. IEICE* 1999; **99**(374): 7.
8. Nagashima K, Kunihiro T, Takayanagi I, Nakamura J, Kosaka K, Yurimoto H. *ITE Tech. Rep.* 2000; **24**(3): 13.
9. Vassos BH, Ewing GW. In *Analog and Digital Electronics for Scientists* (3rd edn). John Wiley: New York, 1985; 501.
10. Gray PR, Meyer RG. In *Analysis and Design of Analog Integrated Circuit* (2nd edn). John Wiley: New York, 1984; 771.
11. Sze SM. In *Semiconductor Devices: Physics and Technology*. John Wiley: New York, 1985; 523.